Available online at www.sciencedirect.com
SCIENCE DIRECT®
Thermochimica Acta 434 (2005) 42–49
thermochimica acta
www.elsevier.com/locate/tca

Surface acidity of catalytic solids studied by base desorption: experimental and modelling approaches

Antonella Gervasini[a,*], Paolo Carniti[a], Aline Auroux[b]

[a] *Dipartimento di Chimica Fisica ed Elettrochimica, Università degli Studi di Milano, via C. Golgi n. 19, I-20133 Milano, Italy*
[b] *Institut de Recherches sur la Catalyse, CNRS, 2 av. A. Einstein, F-69626 Villeurbanne, France*

Received 23 August 2004; received in revised form 25 November 2004; accepted 31 December 2004
Available online 29 January 2005

Abstract

A thermogravimetric analyzer (TGA) was used to collect thermodesorption curves of 2-phenylethylamine (PEA) from acidic surfaces with the aim of determining the amount and distribution of the acid sites of the samples. Oxides widely used as active phase supports as well as catalytic phases were selected for this study: alumina, silica, silica–alumina, silica–zirconia, and silica–titania. The thermodesorption curves were collected at different heating rates ($5 \leq \beta$ (°C/min) ≤ 30) in inert atmosphere. The activation energies of PEA desorption from the acid sites were calculated from the dependence upon the heating rate β of the displacements of the observed desorption peaks (T_{max}) as determined from the derivative of the TGA profiles (DTGA). For a more accurate kinetic study of the desorption phenomenon, a kinetic model based on parallel reactions of desorption, each one running with its own kinetic parameter in a temperature-dependent manner in accordance with Arrhenius's law, was applied to the experimental desorption data at the different heating rates. The quantitative acid site energy distribution was optimized for each sample, and kinetic parameters for each type of acid site were determined. The conclusions drawn from PEA thermodesorption were compared with the results obtained from the differential heat curves of ammonia adsorption measured at 80 °C in a volumetric–calorimetric line.

Keywords: Oxides; Acidity; Thermal desorption; Thermogravimetry; Calorimetry

1. Introduction

Due to the large number of reactions which are catalyzed by acid sites, it is recognized that solid acids are currently the most important solid catalysts [1]. It is therefore of very high importance to study solid acids in terms of the nature, amount, strength and strength distribution of their surface sites, from the fundamental and applicative points of view.

Suitable basic probe molecules are used for the quantitative analysis of the solid acidity, by studying either adsorption from zero coverage to partial or full coverage of the surface, or desorption from surfaces completely saturated by the probe. Spectroscopic techniques are usually employed to elucidate the nature of the molecular complex formed by the basic probe adsorbed on the acid site [2–5], while thermal techniques (i.e., calorimetry, thermogravimetry, temperature-programmed desorption analysis [6–9]) can be used to quantify the thermal effects associated with the acid–base adsorption reaction, which gives a measure of the strength and strength distribution of the acid sites. Thermal desorption techniques have gained a great popularity due to their comparatively easier operation. Various different mathematical analyses of the thermodesorption profiles have been proposed by different authors to provide kinetic information about the distribution of the surface acid strength [10,11]. A simple approach is based on the analysis of thermodesorption curves collected at different heating rates (β). The shift of the temperature of maximum rate of desorption (T_{max}) as a function of β can be exploited to derive activation parameters (i.e., E_a) of the desorption reaction by means of different model equations [12,13]. When heterogeneous solids are concerned, in

* Corresponding author. Tel.: +39 02 50314254; fax: +39 02 50314300.
E-mail address: antonella.gervasini@unimi.it (A. Gervasini).

0040-6031/$ – see front matter © 2005 Elsevier B.V. All rights reserved.
doi:10.1016/j.tca.2004.12.019

order to derive the activation energy distribution of the acid surface, the shift of T_{max} with β has to be considered separately for each peak. However, for this approach to provide a reliable determination of the activation parameters, the thermodesorption curves have to be well defined, with clearly detectable T_{max} values.

The aim of the present study was to characterize the acidity of several oxides chosen among materials widely used as supports for active phases as well as catalytic phases. The oxides were synthesized by sol–gel route, which made it possible to control the texture and composition of the prepared samples. The acidic properties were determined by thermal desorption of 2-phenylethylamine (PEA), chosen as base probe molecule. The experiments were carried out with a thermogravimetric analyzer. The PEA thermodesorption curves, collected at different heating rates, were numerically treated with a novel mathematical model in order to kinetically interpret them and derive the kinetic and activation parameters for each type of acid site of the surface in addition to the amounts of sites of each type. This allowed us to map the acid sites of the surfaces from an energetic point of view, in terms of activation energies for PEA desorption. To corroborate our approach, a conventional acid–base titration by ammonia adsorption was performed in a linked microcalorimetric–volumetric apparatus. In this case, the energy map of the acid sites of the surfaces was obtained in terms of adsorption enthalpies.

2. Experimental

2.1. Sample preparations and measurements

Pure alumina (A) and silica (S), and silicas modified with Al (SA), Ti (ST), and Zr (SZ) were synthesized via sol–gel route, using pure grade reagents from Fluka and Merck–Schuchardt. Tetraethyl orthosilane (TEOS), aluminium triisopropylate, tetraethyl orthotitanate, and zirconium propoxide (solution 70% in propanol) were used as starting materials for Si, Al, Ti, and Zr, respectively. The SA and ST samples were obtained by base-catalyzed hydrolysis of TEOS and aluminium triisopropylate, while SZ was synthesized by acid-catalyzed hydrolysis of TEOS. The synthesis of S, A, SA and ST was carried out using ethyl alcohol (99.8%, v/v), water, and tetrapropylammonium hydroxide solution (20% in water, TPA-OH) as gelling agent; the synthesis of SZ employed 1-propanol, hydrochloric acid as catalyst, and ammonia as gelling agent. The obtained gels were aged for 18 h at room temperature, then dried at 120 °C for 6 h and calcined at 550 °C for 8 h. More details on the preparation procedure and on the surface and bulk properties of the samples as characterized by inductive coupled plasma analysis (ICP), X-ray diffraction analysis (XRD), X-ray photoelectron spectroscopy (XPS), N_2 physisorption, and scanning electron microscopy (SEM) can be found in Ref. [14].

The thermodesorption of 2-phenylethylamine (PEA) from the saturated powders was studied using a TGA 7 Perkin-Elmer thermal analyser. The sample temperature in the 150–600 °C range was calibrated by measuring the Curie transitions (T_C) of high-purity reference materials (alumel, nickel, perkalloy, and iron) at each different heating rate (β) employed. Prior to the desorption analysis, the powders were activated in vacuum for 16 h at 400 °C under a residual pressure of 10^{-3} Torr, then transferred into a glass cell equipped with connections for a vacuum/gas line. PEA (purity > 99% from Fluka) was then introduced, up to complete coverage of the powder. After 3 h at room temperature under N_2 flow, the excess of non-adsorbed PEA was removed by filtration. The obtained saturated powder was loaded on the pan of the TGA apparatus (10–15 mg) and a two-step analysis was performed under N_2 flow (30 ml min^{-1}). The first isothermal step, carried out at 50 °C, removed all the excess PEA from the surface, while the second step was non-isothermal, with a temperature increase from 50 up to 800 °C at a constant heating rate (β = 5, 10, 15, 20, 30 °C/min) in order to completely remove PEA from the surface. The total and intermediate PEA mass losses were determined by subtracting the final mass at 800 °C from the mass measured at the end of the first isothermal step or from the masses at definite times/temperatures of analysis corresponding to well defined steps of the thermogram.

The microcalorimetric measurements of NH_3 adsorption were performed at 80 °C in a heat-flow calorimeter of the Tian-Calvet type (C80 from Setaram) linked to a conventional volumetric apparatus equipped with a capacitance manometer for pressure measurements (Datametrics). Prior to the measurements, the samples (about 0.1 g) were outgassed at 400 °C for 16 h. After a first adsorption, performed by repeatedly adding successive amounts of NH_3 onto the sample until an equilibrium pressure of about 67 Pa was reached, the sample was evacuated for 30 min, to remove the weakly adsorbed NH_3, and a second adsorption was performed.

2.2. Modelling and computations

Once determined the amounts of PEA desorbed (total or intermediate mass losses) during the TGA experiments, the numbers of acid sites (eq/g_{oxide}) could be determined based on the assumption of a base:acid site = 1:1 stoichiometry.

The derivatives of the TGA curves (DTGA) made it possible to determine the times/temperatures at which the maximum rates of PEA desorption occurred (T_{max}). Activation energies for PEA desorption from the different surface sites can be calculated exploiting the observed shifts of the T_{max} values with β by using the Kissinger equation [15]:

$$\beta E_a / RT_{max}^2 = A\alpha(1-x)_{max}^{\alpha-1} \exp(-E_a/RT_{max}) \quad (1)$$

where R is the gas constant, A the pre-exponential factor of the Arrhenius equation, α the reaction order (in the present

Table 1
Composition and properties of the samples

Label	Oxide	Composition (wt.%)	S (m^2/g)	Vp (cm^3/g)	Acid sites (meq/g)	
					From PEA[a]	From NH_3[b]
S	SiO_2	100	387	1.04	0.187	0.054
A	Al_2O_3	100	244	1.60	0.302	0.437
SA	SiO_2–Al_2O_3	12.2 (Al_2O_3)	777	0.86	0.503	0.480
ST	SiO_2–TiO_2	13.2 (TiO_2)	494	0.69	0.183	0.307
SZ	SiO_2–ZrO_2	14.3 (ZrO_2)	596	1.69	0.309	0.374

[a] Determined by PEA thermodesorption associated with $T_{max,2}$ peak (second-step analysis, desorption from 50 to 800 °C).
[b] Determined at 0.2 Torr of NH_3 coverage.

case, the order of the desorption reaction), and x the fraction reacted (in the present case, the fraction desorbed). The equation can be easily linearized independently of the order. Thus, by plotting $\ln(\beta/T_{max}^2)$ versus $1/T_{max}$, E_a values for each T_{max} detected can be obtained from the slopes of the linear-regression straight lines.

For a better kinetic interpretation of the desorption reaction data, we applied a mathematical model which regards PEA desorption as the result of different simultaneous independent first-order reactions, each one relevant to a single type of site. All the desorption reactions were considered to follow Arrhenius' law [14]. All the surface sites able to chemically retain the amine were supposed to be saturated at the beginning of the temperature-programmed desorption. Due to the texture of the samples, there was no obstruction to removal of the amine once broken the bond with the acid site, which makes it unnecessary to consider the readsorption of the desorbed amine molecules. For the kinetic modelling, the experimental TGA profiles were interpreted up to 600 °C, as higher temperatures caused morphologic and structural damages to some samples [14].

A set of differential equations, containing all the kinetic equations of desorption from each type of site, was written. The equations were numerically integrated by a fourth-order Runge–Kutta method [16]. The parameters of the model were optimized by minimizing the sum of the squares of the differences between the calculated and experimental PEA residual fractions on the surface at time t_j and heating rate β_k ($x_{calcd,j,k}$ and $x_{exptl,j,k}$, respectively). The parameters to be determined were: n, the number of different types of sites on the surface; x_i^0 ($i = 1,2,\ldots,n$), the residual fraction of PEA on the ith type of site at time zero, corresponding to the fraction of sites of ith type; and the Arrhenius parameters, namely the pre-exponential term A_i, and the activation energy $E_{a,i}$ for each type of site. As the maximum value of n considered was 4, the maximum number of parameters to be optimized at the same time was 11. The very high number of experimental points (from 670 to 1155 distributed on 4 or 5 different heating rates (β) for each sample) guaranteed the possibility of attaining sound parameters. The indicative values obtained by the Kissinger approach were employed as starting values for the parameters to be optimized.

3. Results and discussion

Table 1 shows the composition and properties of the calcined samples prepared by sol–gel. The surface areas and pore volumes of the samples were determined by N_2 adsorption/desorption isotherms at −196 °C. The surface areas of the modified silicas (SA, ST, and SZ) were higher than those of pure silica and alumina. As the samples underwent very high temperatures (up to 800 °C), higher than that of calcination, during the basic probe desorption experiments, their morphologic and structural stability was controlled. As a general trend, a less or more definite decrease of surface area was observed for all the samples upon very high temperature heating [14]. SZ and SA maintained high surface area (293 and 210 m^2/g, respectively) following heat treatment at 900 °C for 8, while a more decisive decrease in surface area was observed for the ST and S samples. Moreover, the amorphous character of the powders was maintained in every case also following high thermal treatments, as confirmed by XRD analysis. Only pure silica was quite completely converted to cristobalite structure upon treatment of 900 °C [14]. XPS spectroscopy confirmed the presence of Al, Ti, and Zr on the modified silica surfaces [14], guaranteeing a proper modification of the surface acidity of the samples compared with that of pure silica.

To characterize the surface acidity of the samples, we studied the thermal desorption of PEA in a thermogravimetric apparatus (TGA) and NH_3 adsorption experiments, carried out in a volumetric–microcalorimetric line, were also performed to corroborate the results. The basic probes used, PEA and NH_3, have strong basicity ($pK_{a,NH_3} = 9.25$; $PA_{NH_3} = 858$ kJ/mol and $pK_{a,PEA} = 9.84$; $PA_{PEA} = 936.2$ kJ/mol) and different sizes ($d_{NH_3} = 4.2$ Å and $d_{PEA} = 7.0$ Å). PEA has already been used as a probe for titrating the acidity of catalytic solids in solution (aqueous or organic) by a pulse-liquid chromatographic technique utilizing a UV-detector ($\lambda = 254$ nm) [17]. For thermogravimetric measurements, PEA is particularly useful due to its high molecular mass ($M = 121.18$ g/mol). Very numerous and important reports can be found in the literature on the use of thermal desorption [18–20] and calorimetric adsorption of basic probes [21–24] for the study of solid acidity. The comparison between the obtained results from the two approaches can be hard but very informative.

3.1. PEA thermodesorption

The clean and activated surfaces were placed in contact with liquid PEA, thus achieving complete saturation of the acid sites. The saturated and dried powders were then subjected to a two-step TGA analysis as described in the experimental section and illustrated in Scheme 1. The first isothermal step (50 °C) was aimed at desorbing the excess multi-layer of PEA deposited on the surface. In every case, a constant value of the mass was eventually obtained, with a well-defined plateau versus analysis time. The mass obtained at the plateau corresponded to the initial mass of the sample under study covered by a monolayer of PEA. The second step of analysis was carried out by increasing the temperature from

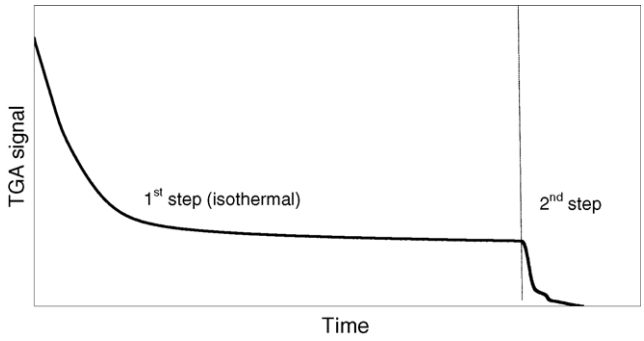

Scheme 1. Two-step TGA analysis performed to study the surface acidity of the sample surfaces: 1st step is carried out at 50 °C and 2nd step at increasing temperature from 50 to 800 °C.

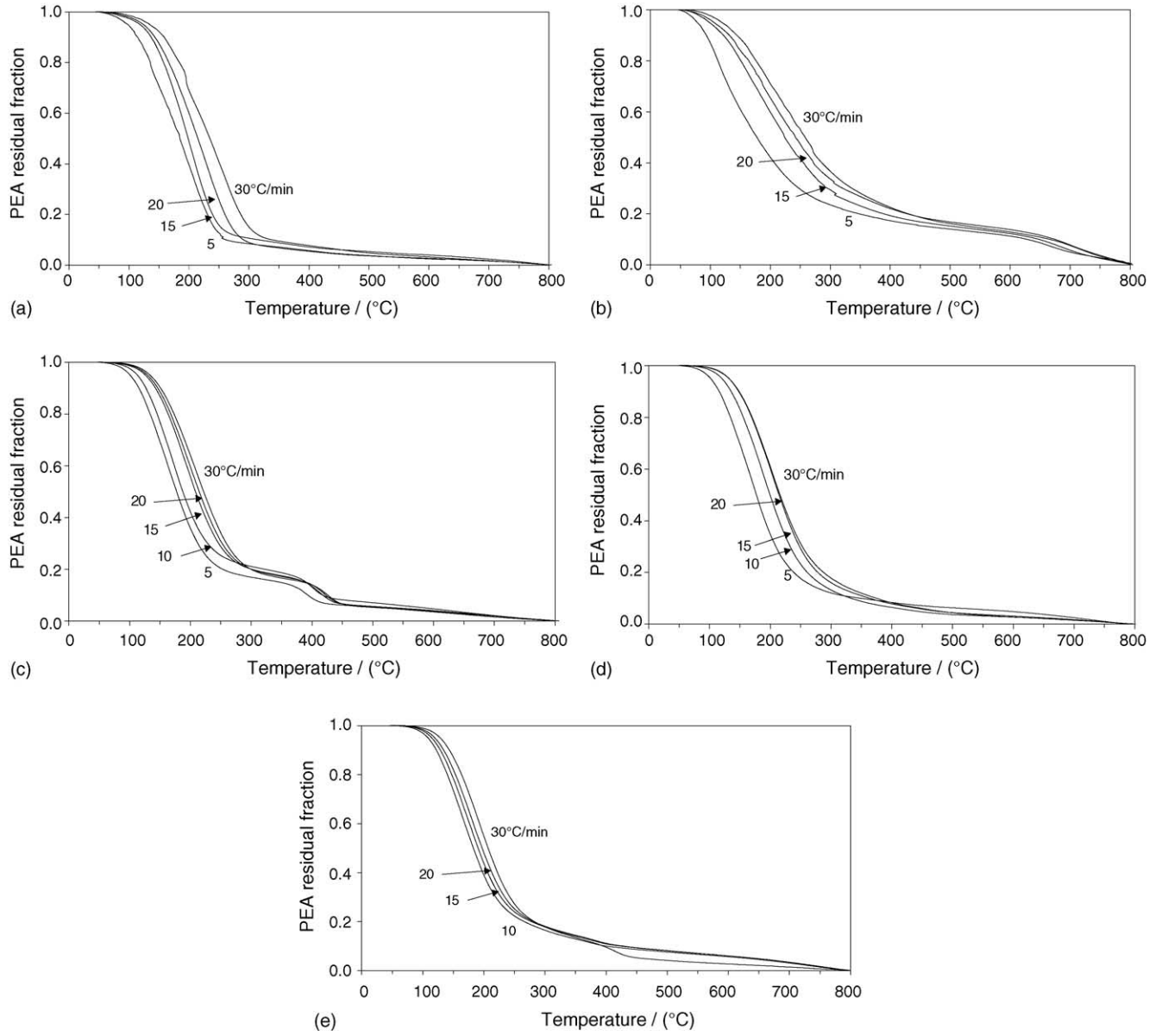

Fig. 1. Experimental thermogravimetric curves of PEA desorption from saturated samples as a function of temperature (second-step analysis) at the different heating rates (β, °C/min): (a) silica, S; (b) alumina, A; (c) silica–alumina, SA; (d) silica–titania, ST; (e) silica–zirconia, SZ.

50 up to 800 °C at constant rate (from 5 up to 30 °C/min) to completely desorb PEA. The final mass obtained at 800 °C corresponded to the catalyst mass for which the amounts of acid sites were determined.

Fig. 1a–e reports the thermograms for PEA desorption from each sample, collected at various heating rates (β) and reconstructed by plotting the residual fraction of PEA against sample temperature from 50 to 800 °C. All the curves are decreasing down to zero. As a general trend, the curves obtained at lower values of β lay below those obtained at higher β. This trend is particularly noticeable up to a residual fraction of PEA of 0.1 (Fig. 1a–e). This behaviour was expected, as for higher values of the heating rate β the sample remained for a shorter time at a defined temperature, thus allowing only a smaller fraction of PEA to desorb. The total amount of PEA desorbed and, therefore, the total amount of acid sites irrespective of acid strength, could be directly obtained from the height of the TGA plateau at 50 °C, corresponding to the end of the first isothermal step: the respective values were 2.94 meq/g (SZ), 2.75 meq/g (SA), 2.13 meq/g (A), 1.79 meq/g (ST), and 1.87 meq/g (S).

When one compares the PEA thermodesorption curves of the different samples, well different shapes of the curves are observed, reflecting the different acid site distributions of the surfaces. The first derivative of the TGA curves (DTGA) highlighted the inflection points as negative peaks, clearly evidencing the temperature at which the rate of PEA desorption went through a maximum (T_{max}). For some samples, more than one peak was observed, indicating that more than one type of acid site was present on the surface, with different acid strengths. The conventional view is that the lowest values of T_{max} correspond to the weakest acid sites.

Two distinct T_{max} values were observed with A, SA, ST, and SZ, and only one with S. The $T_{max,1}$ values (170–220 °C) associated with a first type of site are in all cases near the boiling temperature of PEA (T_b = 198–200 °C at atmospheric pressure). The amount of PEA desorbed at $T_{max,1}$, which is indicative of PEA weakly bound to the surface sites, corresponded to 80–90% of the total amine desorbed. The fraction of PEA associated with the maximum desorption at higher temperature ($T_{max,2}$, 360–460 °C) was smaller for S and ST than for A, SZ, and SA (Table 1). Fig. 2 reports for the SZ sample, as an example, three DTGA curves as a function of temperature calculated from the relevant TGA profiles collected at 5, 10, and 15 °C/min. The shift of the main peak at low temperature, $T_{max,1}$, with β can be clearly individuated, while another peak at higher temperature, $T_{max,2}$, is better detected as higher β is. In this case, it is hard to detect a clear shift of $T_{max,2}$ with β.

The activation energies for PEA desorption from the different detected acid sites have been calculated by the Kissinger equation [15]. On the basis of this equation (Eq. (1)), E_a values can be calculated for each T_{max} detected from the slope of the straight lines obtained by plotting $\ln(\beta/T_{max}^2)$ versus $1/T_{max}$. As a general trend, E_a values similar to the enthalpy of PEA vaporization (ΔH_v = 42 kJ/mol) were obtained

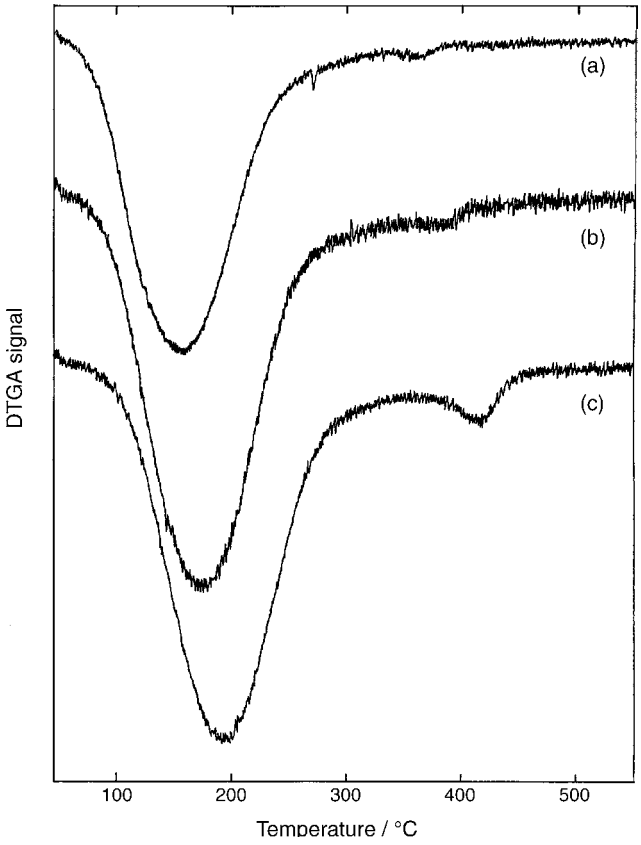

Fig. 2. DTGA curves calculated from the TGA profiles of PEA thermodesorption from SZ surface collected at heating rate of 5 °C/min (a), 10 °C/min (b), and 15 °C/min (c).

for the acid sites associated with $T_{max,1}$; meanwhile, values of 68, 97, 108, and 269 kJ/mol, associated with $T_{max,2}$, were obtained for ST, SZ, SA, and A, respectively. However, E_a values obtained in this manner may be of little significance, as convoluted DTGA peaks were observed in most cases. In this situation, the shift of T_{max} with β could not be determined accurately, and moreover it is likely that more than two types of acid sites are present.

To achieve a better kinetic interpretation of the PEA desorption curves, a mathematical model was applied to the experimental data taking into account at the same time the experiments performed at the different heating rates. Only the temperature interval from 50 to 600 °C was utilized in the computations because of a significant, even if moderate, loss of surface area occurring at higher temperatures [14].

The optimum parameters determined using these computations (n, x_i, x_i^0, A_i, $E_{a,i}$, see Section 2.2) can be used to recalculate all the thermograms. The fitting with the experimental curves was of good quality: the calculated desorbed fractions were well inside a ±10% deviation from the experimental values, and no particular trend with β could be observed. This determination of the parameters of the model makes it possible to decompose the PEA thermodesorption curves into single curves, each relevant to a different type of

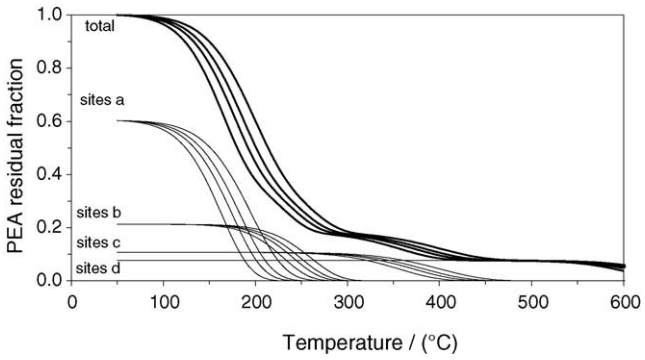

Fig. 3. Decomposition of the calculated curves of PEA thermodesorption (total) of SZ surface for the different types of acid sites, calculated at the different heating rates (curves at lower β are below those obtained at higher β).

acid site. In this way, it is possible to follow the PEA desorption from each type of site. Fig. 3 shows, as an example, the numerical decomposition of the experimental thermograms into four calculated curves, corresponding to the four types of acid sites of the SZ surface. The curves have been calculated for all the heating rates used in the experiments. The curve decomposition highlights the occurrence of both successive and simultaneous desorptions of the amine molecule from the different surface sites: PEA can desorb from the various populations of sites from weakest to strongest consecutively as well as simultaneously. In the second case, PEA desorption from a given type of site begins to occur before desorption from other types of sites is complete.

The calculated distributions of activation energies for PEA desorption from the acidic surfaces are shown in Fig. 4. The different types of acid sites have been grouped into sites with E_a values smaller than 60 kJ/mol, E_a between 60 and 100 kJ/mol, between 100 and 200 kJ/mol, and E_a greater than 200 kJ/mol. Pure silica and alumina have only two types of sites. Restricting oneself to the sites with E_a higher than 60 kJ/mol, S has only one type of site, with a low E_a value between 60 and 100 kJ/mol, while A presents sites with very high E_a value (higher than 200 kJ/mol). The acidity of the modified silica surfaces (SA, ST, and SZ) was very different. SA and SZ have surfaces with very high amounts of acidic sites and different acidic strengths ($60 < E_a < 200$ kJ/mol), while ST has a poorly acidic surface presenting only a small amount of sites of high acidic strength.

The site energy distribution of the oxide surfaces determined using the model better represents the heterogeneity of the surfaces than the direct interpretation of the experimental thermal desorption data.

3.2. NH_3 adsorption

The integral and differential heats evolved from NH_3 adsorption measured at 80 °C, up to 0.5 Torr of NH_3 coverage, are shown in Figs. 5 and 6 for all the samples. Integral heat curves for the A, SA, and SZ samples run together, while ST has a curve well below those of the three other samples (Fig. 4). The curves can be approximately viewed as sections of parabolas, and the highest parabola corresponds to the sample on which the titration of the largest amount of strong sites occurred [25]. This suggests that the A, SA, and SZ samples have surfaces with the highest acidity in terms of number and strength of the sites. The plots of differential heats versus coverage (Fig. 6) make it possible to study the distribution of the acid sites on the different surfaces. Initial heats for the A and SA samples at very low NH_3 coverages are very high, 270 and 180 kJ/mol, respectively. Continuously decreasing curves are observed for A and SA without a clearly detectable plateau in the whole range of the heats measured. This behaviour is typical of highly heterogeneous surfaces. For SZ, it is possible to individuate a first plateau in the 150–140 kJ/mol region for a wide range of NH_3 coverage, and a second one close to 90 kJ/mol at higher NH_3 coverage. The surface acidity of the ST sample is rather low, in terms of both the amount of acid sites and the acidic strength; two plateaux, around 85–90 and 65–70 kJ/mol, respectively, could be identified. Pure silica did not exhibit any acidity, as expected.

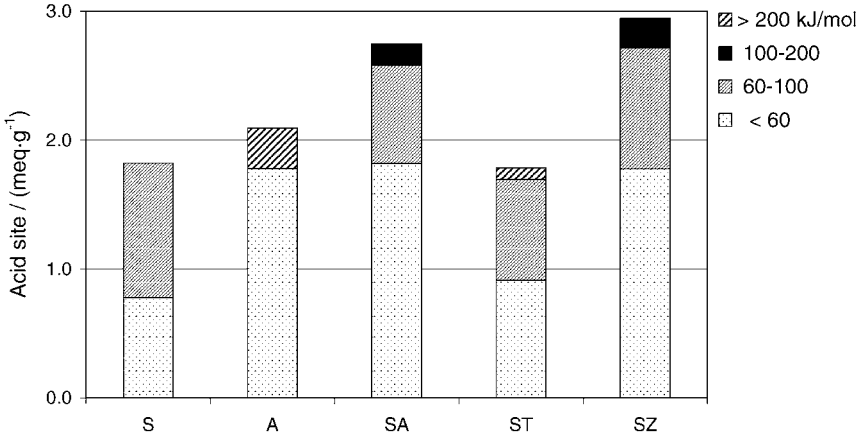

Fig. 4. Calculated distribution of activation energies for PEA desorption from the different types of acid sites of the studied oxides.

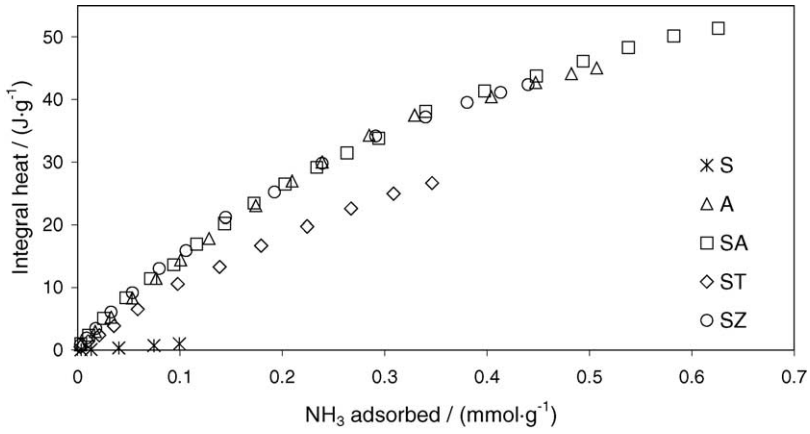

Fig. 5. Integral heats of NH_3 adsorption as a function of NH_3 coverage, measured at 80 °C.

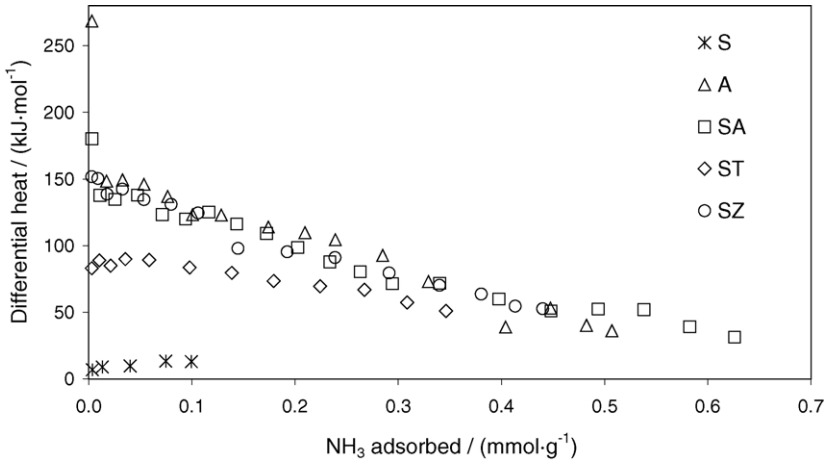

Fig. 6. Differential heats of NH_3 adsorption as a function of NH_3 coverage, measured at 80 °C.

The amount of strong acid sites retaining NH_3 can be evaluated by determining the amount of NH_3 adsorbed at 0.2 Torr, from the adsorption isotherms (Table 1). SA has a higher number of acid sites than A (9%), SZ (25%), and ST (44%). During the adsorption experiments, the different types of acid sites are covered successively, starting with the strongest ones (highest adsorption enthalpy), according to the conventional view. This does not take into account the real possibility of simultaneous adsorption on different types of sites with different enthalpies, which can occur more or less markedly depending on adsorption temperature [26]. In the present case, since very low NH_3 coverage was investigated, not all the acidic sites of the surfaces were involved in the adsorption process, and titration by NH_3 concerned almost exclusively the strong acid sites.

Differences are usually reported in the literature when comparing the numbers of surface acid sites derived from different experimental methodologies [27]. The differences can often be ascribed to different experimental conditions used in some pre-treatment stage or analysis. In the present case, when comparing the results obtained by PEA thermodesorption with those derived from NH_3 adsorption, satisfactory agreement is found between the amounts of strong acidic sites determined from the desorption profiles (site fractions associated with the $T_{max,2}$ peak) and those titrated by ammonia (Table 1). Concerning the acid strength of the oxide surfaces, the distribution of adsorption enthalpies obtained by NH_3 adsorption indicates the same order of acidity as that obtained by the model applied to the thermal desorption curves in terms of activation energy of PEA desorption.

4. Conclusions

We have investigated the acidity of various oxide surfaces using NH_3 or PEA as basic probes. The direct comparison of the two series of experimental data based on base probe desorption or adsorption provided a sound interpretation of the acid site energy distribution of the surfaces from a qualitative and quantitative point of view. A kinetic model applied to the PEA desorption profiles gave access to the distribution of the surface acid sites taking into account their number and energy (activation energy of amine desorption). The results obtained from the computation are in good agreement with

those derived from the ammonia adsorption approach, when the comparison is confined to the strong fraction of acid sites.

Acknowledgements

The authors want to thank Dr. Simona Bennici (Dipartimento di Chimica Fisica ed Elettrochimica, Università di Milano, Italy) for assistance with the experiments.

References

[1] A. Corma, Chem. Rev. 95 (1995) 559.
[2] M.C. Kung, H.H. Kung, Catal. Rev.-Sci. Eng. 27 (1985) 425.
[3] A. Auroux, A. Gervasini, C. Guimon, J. Phys. Chem. 103 (1999) 7195.
[4] R. Borade, A. Sayari, A. Adnot, S. Kaliaguine, J. Phys. Chem. 94 (1990) 5989.
[5] J.F. Haw, I.S. Chuang, B.L. Hawkins, G.E. Maciel, J. Am. Chem. Soc. 105 (1983) 7206.
[6] V. Solinas, I. Ferino, Catal. Today 41 (1998) 179.
[7] A. Auroux, Topics Catal. 4 (1997) 71.
[8] R.J. Gorte, Catal. Today 42 (1988) 239.
[9] H.G. Karge, V. Dondur, J. Phys. Chem. 94 (1990) 765.
[10] F. Arena, R. Dario, A. Parmaliana, Appl. Catal. A: Gen. 170 (1998) 127.
[11] J.M. Kanervo, K.M. Reinikainen, A.O.I. Krause, Appl. Catal. A: Gen. 258 (2004) 135.
[12] J.H. Chan, S.T. Balke, Polym. Degrad. Stabil. 57 (1997) 135.
[13] Z.S. Petrović, Z.Z. Zavargo, J. Appl. Polym. Sci 32 (1986) 4353.
[14] P. Carniti, A. Gervasini, S. Bennici, J. Phys. Chem. B 109 (2005) 1528.
[15] H.E. Kissinger, Anal. Chem. 29 (1957) 1702.
[16] E. Cano-Serrano, G. Blanco-Brieva, J.M. Campos-Martin, J.L.G. Fierro, Langmuir 19 (2003) 7621.
[17] P. Carniti, A. Gervasini, Presented at the Fifth European Congress on Catalysis, EUROPACAT-V, Limerick, Ireland, September 2–7, 2001.
[18] H.G. Karge, V. Dondur, J. Weitkamp, J. Phys. Chem. 95 (1991) 283.
[19] H.J. Kreuzer, Langmuir 8 (1992) 774.
[20] M.C. Abello, A.P. Velasco, M.F. Gomez, J.B. Rivarola, Langmuir 13 (1997) 2596.
[21] A. Gervasini, A. Auroux, J. Phys. Chem. 94 (1990) 6372.
[22] A. Gervasini, G. Bellussi, J. Fenyvesi, A. Auroux, J. Phys. Chem. 99 (1995) 5117.
[23] A. Gervasini, J. Fenyvesi, A. Auroux, Langmuir 12 (1996) 5356.
[24] N. Cardona-Martínez, J.A. Dumesic, J. Catal. 127 (1991) 706.
[25] A. Gervasini, A. Auroux, J. Phys. Chem. 97 (1993) 2628.
[26] P. Carniti, A. Gervasini, A. Auroux, J. Catal. 150 (1994) 274.
[27] J. Zajac, R. Dutartre, D.J. Jones, J. Rozière, Thermochim. Acta 379 (2001) 123.